

---

# Combining Constrained Diffusion Models and Numerical Solvers for Efficient and Robust Non-Convex Trajectory Optimization

---

Anjian Li<sup>1</sup>, Zihan Ding<sup>1</sup>, Adji Bousso Dieng<sup>2,3</sup>, Ryne Beeson<sup>4</sup>

<sup>1</sup>Department of Electrical and Computer Engineering, Princeton University

<sup>2</sup>Department of Computer Science, Princeton University

<sup>3</sup>Vertaix

<sup>4</sup>Department of Mechanical and Aerospace Engineering, Princeton University

## Abstract

Motivated by the need to solve open-loop optimal control problems with computational efficiency and reliable constraint satisfaction, we introduce a general framework that combines diffusion models and numerical optimization solvers. Optimal control problems are rarely solvable in closed form, hence they are often transcribed into numerical trajectory optimization problems, which then require initial guesses. These initial guesses are supplied in our framework by diffusion models. To mitigate the effect of samples that violate the problem constraints, we develop a novel constrained diffusion model to approximate the true distribution of locally optimal solutions with an additional constraint violation loss in training. To further enhance the robustness, the diffusion samples as initial guesses are fed to the numerical solver to refine and derive final optimal (and hence feasible) solutions. Experimental evaluations on three tasks verify the improved constraint satisfaction and computational efficiency with  $4\times$  to  $30\times$  acceleration using our proposed framework, which generalizes across trajectory optimization problems and scales well with problem complexity.

## 1 Introduction

Optimal control problems are fundamental in decision-making for autonomous agents including self-driving cars, robot manipulators, and spacecraft trajectories to name just a few. In the open-loop case, with a predetermined initial configuration, the goal is to plan an optimal path and control history for an agent to reach a target while satisfying the dynamics and safety constraints. These problems often have non-convex structure, which may be due to complex nonlinear system dynamics and environmental constraints. Ultimately, this results in multiple minima and solutions that may have different qualitative behavior with various tradeoffs. Identifying these diverse and locally optimal (and hence feasible) solutions efficiently remains a significant challenge in the field.

The open-loop optimal control problem can be cast as a numerical trajectory optimization problem using a variety of approaches [4]. When the optimal control problem involves nonlinear functions, this often results in a nonlinear program (NLP) where an initial guess is required to get the solution. In the case where one is interested in solving for several solutions, a global search is needed. This is essentially a two-step process: (i). sampling a distribution on the control space, and (ii). using this sample as an initial guess to the NLP solver that hopefully generates a solution. For each solution from the NLP, optimality (and hence feasibility) is often verified by the solver by checking whether the first order necessary conditions, the Karush-Kuhn-Tucker (KKT) conditions, are satisfied [29, 25].

However, the high dimensionality and non-convex nature of the problem often make the two-step global search process time-consuming and cannot satisfy the efficiency demands of autonomous systems.

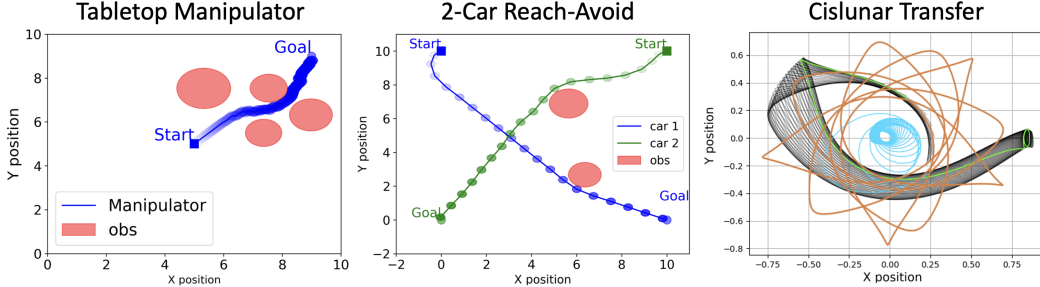


Figure 1: Three trajectory optimization tasks in our experiments (from left to right): *tabletop manipulation* (161 DoF); *two-car reach-avoid* problem (81 DoF); *cislunar transfer* problem (64 DoF). The degree-of-freedom (DoF) indicates the dimension of control variables for each task.

Machine learning has also gained popularity in trajectory optimization, like warm starting the convexified trajectory optimization problems such as Quadratic Programming (QP) [11, 9, 38]. These approaches primarily focus on predicting a single solution to the QP problem to improve the computational efficiency, rather than modeling the distribution of diverse solutions to the original non-convex problem. Recently, generative models, particularly diffusion models, have shown good performance in generating trajectories or controls from a distribution [24, 1, 12, 8, 42]. When conditioned on the environmental parameters, diffusion models can efficiently generate appropriate and diverse trajectories even in *a priori* unknown environment. However, the diffusion model output trajectories are not robust to prediction error and may violate the dynamic and safety constraints, which can cause catastrophic damage to safety-critical systems. It’s also difficult for the diffusion model to directly output locally optimal trajectories. While efforts have been made to integrate safety constraints into generative models [32, 10, 49, 48, 36, 6], it is still challenging to achieve solution quality, computational efficiency, diversity, robustness and feasibility.

In this paper, we propose a general framework for efficient non-convex trajectory optimization with enhanced robustness for constraint satisfaction. This framework creates a synergy between a novel constrained diffusion model and a numerical optimization solver. We first formulate the trajectory optimization problem as a nonlinear program, where a numerical solver can be used to collect solutions as training data. Then we train a conditional diffusion model to efficiently sample a set of diverse and high-quality trajectory predictions, from which the solver can fine-tune to obtain final solutions with enhanced feasibility and optimality. We also developed an innovative constrained diffusion model that incorporates an additional constraint violation loss in the training process to minimize the violation in the samples.

Our framework has the following appealing properties: **(a). Computational Efficiency.** Trained with offline solution data, the diffusion model can predict high-quality solutions that are close to local optima and warm-start the trajectory optimization. This significantly accelerates the solver convergence with considerable computational time savings. **(b). Robustness (Constraint Satisfaction).** We used a constrained diffusion model specifically designed to produce samples with minimal constraint violations. These sampled trajectories are then further refined by a numerical solver to enhance the feasibility and optimality. **(c). Automatic Data Generation.** With a numerical solver, we can automatically generate diverse problems and collect corresponding solutions, which allows for on-demand data augmentation whenever required. **(d). Generalization.** Our framework is suitable for trajectory optimization across various applications with flexible environment settings.

We demonstrate the efficacy of our framework on three non-convex trajectory optimization problems for open-loop optimal control: *tabletop manipulation*, *two-car reach-avoid*, and *cislunar low thrust transfer* for a spacecraft. Our framework improves the efficiency of obtaining solutions compared to the baseline while enhancing constraint satisfaction.

## 2 Related Work

**Machine Learning for Optimization.** Machine learning methods have been widely used to solve a variety of optimization problems with different techniques, including convex Quadratic Programming (QP) [50, 51, 11, 38], mixed-integer programming [9], combinatorial optimization [43, 23] and black-box optimization [30, 45, 28], etc. To improve the constraint satisfaction in optimization problems, neural networks have been incorporated with fully differentiable constraint function [16]. Conditional variational autoencoder (CVAE) and long short-term memory (LSTM) are proposed to warm-start the general nonlinear trajectory optimization problems [32]. Another branch of work leverages machine learning methods and pre-collected solution data points for solving partial differential equations (PDEs) [7]. One of the most popular work is physics-informed neural networks (PINN) [37], which introduces the solution prediction model with a hybrid training loss for labeled solution prediction and violation of the original PDEs.

**Diffusion Models.** The diffusion models [39, 41] is able to sample the multi-modal distribution with a stochastic differential equation (SDE). The models are further developed into denoising diffusion probabilistic models (DDPM) [21], denoising diffusion implicit models (DDIM) [40] for application of image generation. Both classifier-guided diffusion [13] and classifier-free guidance [22] are proposed to achieve conditional generation with diffusion models. Given the strong expressiveness of the diffusion model, its application has been extended across domains from image generation to reinforcement learning [46, 14, 15], motion generation [44], robotics [12], etc.

**Diffusion-based Trajectory Generation.** Diffusion models are becoming popular in robotics for generating controls or trajectories [1, 24, 33, 42, 12, 34, 15]. Many efforts have been made to improve the diffusion model for creating safe trajectories for safety-critical systems. Control barrier functions [48, 6] and collision-avoidance kernels [10] are employed to guide diffusion models to sample feasible trajectory solutions. To adapt to new constraints in testing, prior work investigated composing diffusion models to improve the generalizability [36, 49]. However, solely relying on diffusion-sampled trajectories will inevitably face the robustness issue of constraint violations and hardly achieve locally optimal solutions. There has been an effort to combine diffusion models with an inference-based trajectory optimization framework [36, 35], but it is not parallelizable and requires extensive computational effort for complex problems. Our work guides the diffusion model toward low constraint violation in the output through a novel loss function and combines it with a fully parallelizable numerical optimization method that scales well.

## 3 Preliminaries

**Non-Convex Trajectory Optimization.** We consider a general open-loop optimal control problem: assume a known agent’s dynamical model, the predefined initial configuration, and the obstacle settings, we aim to plan an optimal trajectory and controls for the agent to reach a target while satisfying the dynamics and safety constraints. With the direct transcription [4], this trajectory optimization problem can be discretized as the following nonlinear program  $\mathcal{P}_y$ :

$$\mathcal{P}_y := \begin{cases} \min_x & J(x;y) \\ s.t., & g_i(x;y) \leq 0, i = 1, 2, \dots, l \\ & h_j(x;y) = 0, j = 1, 2, \dots, m \end{cases} \quad (1)$$

where  $x \in \mathcal{X} \subset \mathbb{R}^n$  is the decision variable to be optimized, and  $y \in \mathcal{Y} \subset \mathbb{R}^k$  represents various problem parameters.  $J \in C^1(\mathbb{R}^n, \mathbb{R}^k; \mathbb{R})$  is the objective function. Each  $h_i \in C^1(\mathbb{R}^n, \mathbb{R}^k; \mathbb{R})$  and  $g_j \in C^1(\mathbb{R}^n, \mathbb{R}^k; \mathbb{R})$  are equality and inequality constraint functions, respectively. In trajectory optimization,  $x$  might include a sequence of control  $u$ , the time variable  $t$  required to reach the target, etc. Parameters  $y$  can include control limits, target and obstacle characteristics such as position and shape, and other relevant factors. The objective function  $J$  can be time-to-reach, fuel expenditure, etc. The constraint functions  $g$  and  $h$  could contain requirements for dynamical models, goal-reaching, obstacle avoidance, etc.

When the problem parameter  $y$  is fixed,  $\mathcal{P}_y$  in Eq. (1) typically presents a non-convex optimization problem with multiple local optima. To solve this problem  $\mathcal{P}_y$ , a gradient-based numerical solver  $\pi$  can be used. A local optimum  $x^*$  to  $\mathcal{P}_y$  is verified by the solver  $\pi$  that satisfies the KKT conditions

(i.e., no constraint violation). To find different  $x^*$ , the user first provides multiple initial guesses  $x^0$  for the decision variables  $x$  to the solver  $\pi$ , typically drawn from a uniform distribution or some heuristic approach. Then the solver  $\pi$  performs an iterative, gradient-based optimization until a local optimum  $x^*$  is found. The popular methods to conduct such gradient-based optimization in non-convex problems include the Interior Point Method (IPM) [47] and the Sequential Quadratic Programming (SQP) [5].

**Diffusion Probabilistic Model.** As expressive generative models, the diffusion probabilistic models [39, 21, 41] generate samples from random noises through an iterative denoising process. The forward process (i.e., diffusion process) iteratively adds Gaussian noise to sample  $x_k$  at the  $k$ -th step according to the following equation:

$$q(x_{k+1}|x_k) = \mathcal{N}(x_{k+1}; \sqrt{1-\beta_k}x_k, \beta_k \mathbf{I}), \quad 0 \leq k \leq K-1. \quad (2)$$

where  $\beta_k$  is a given variance schedule. With the diffusion steps  $K \rightarrow \infty$ ,  $x_K$  becomes a random Gaussian noise. From above one can write:

$$x_k = \sqrt{\bar{\alpha}_k}x_0 + \sqrt{1-\bar{\alpha}_k}\varepsilon, \quad (3)$$

where  $\bar{\alpha}_k = \prod_{k'=1}^k (1-\beta_{k'})$  and  $\varepsilon \sim \mathcal{N}(0, \mathbf{I})$  is a random sample from a standard Gaussian. The data generation process is the reverse denoising process that transforms random noise to data sample:

$$p_\theta(x_{k-1}|x_k) = \mathcal{N}(x_{k-1}; \mu_\theta(x_k), \sigma_k \mathbf{I}), \quad 1 \leq k \leq K \quad (4)$$

with initial noisy data sampled from a random Gaussian distribution  $x_K \sim \mathcal{N}(0, \mathbf{I})$ .  $p_\theta$  is the parameterized sampling distribution, and it can be optimized through an alternative  $\varepsilon_\theta(x_k, k)$  which is to predict  $\varepsilon$  injected for  $x_k$ , for every diffusion step  $k$ . For conditional generation modeling, a conditional variable  $y$  is added to both processes  $q(x_{k+1}|x_k, y)$  and  $p_\theta(x_{k-1}|x_k, y)$ , respectively. The classifier-free guidance [22] can be applied to further promote the conditional information, which learns both conditioned and unconditioned noise predictors as  $\varepsilon_\theta(x_k, k, y)$  and  $\varepsilon_\theta(x_k, k, \emptyset)$ . Specifically,  $\varepsilon_\theta$  is optimized with the following loss function:

$$\mathcal{L}_{\text{diff}} = \mathbb{E}_{(x_0, y) \sim \mathcal{X} \times \mathcal{Y}, k, \varepsilon, b} \left\| \varepsilon_\theta(x_k(x_0, \varepsilon), k, (1-b) \cdot y + b \cdot \emptyset) - \varepsilon \right\|_2^2 \quad (5)$$

where  $x_0$  and  $y$  are sampled from groundtruth data,  $\varepsilon \sim \mathcal{N}(0, \mathbf{I})$ ,  $k \sim \text{Uniform}(1, K)$ ,  $b \sim \text{Bernoulli}(p_{\text{uncond}})$  with given unconditioned probability  $p_{\text{uncond}}$ , and  $x_k$  follows Eq. (3).

## 4 Methodology

In this section, we first proposed the general framework for efficient and robust non-convex trajectory optimization using diffusion models and numerical solvers. Then we introduce a novel constrained diffusion model specifically designed to guide the diffusion models to generate feasible solutions.

### 4.1 A General Trajectory Optimization Framework

It has been observed that for similar trajectory optimization problems  $\mathcal{P}_y$  in Eq. (1), their solutions  $x^*$  often exhibit similar structures [2, 32]. Similar problems are those  $\mathcal{P}_y$  with the same objective  $J$  and constraints  $g, h$ , but with different parameters  $y$ . Thus, the key insight of our framework is to use a diffusion model to learn  $p(x^*|y)$ , the conditional probability distribution of locally optimal solutions, based on pre-solved similar problems. Then the diffusion model can generalize and predict diverse solutions  $\tilde{x}_{\text{new}}^*$  to new scenarios where the condition  $y_{\text{new}}$  value is unseen.

However, diffusion models inevitably make prediction errors, which can result in constraint violations. To address this, we use diffusion samples  $\tilde{x}_{\text{new}}^*$  as initial guesses for the numerical solver, which fine-tunes them to derive the final solutions  $x_{\text{new}}^*$ , increasing both feasibility and optimality. This approach acts like a safety net, enhancing the robustness of the solutions.

We illustrate our proposed data-driven trajectory optimization framework with diffusion models in Fig. 2. In the offline data generation process, we use a numerical solver  $\pi$  to collect locally optimal solutions  $x^*$  for various problem instances  $\mathcal{P}_y$  with uniformly sampled initial guesses. The solutions with sub-optimal objective values are filtered out manually and the remaining dataset is used as the training data. We train a conditional diffusion model to learn  $p(x^*|y)$  with classifier-free guidance

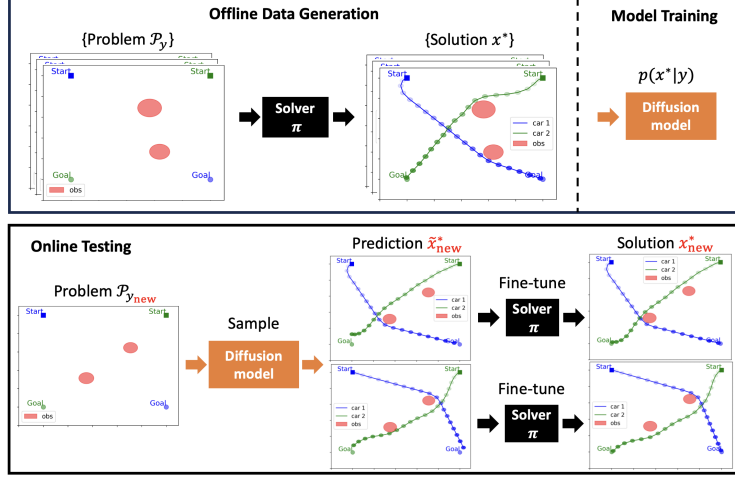


Figure 2: The proposed general framework for non-convex trajectory optimization with a constrained diffusion model and a numerical solver.

[22]. In the online testing process when a new problem  $\mathcal{P}_{y_{\text{new}}}$  is presented with *a priori* unknown value  $y_{\text{new}}$ , we first use the diffusion model to predict diverse solution candidates  $\tilde{x}_{\text{new}}^*$  as initial guesses. Then the numerical solver  $\pi$  only requires minor adjustments to derive the final solutions  $x_{\text{new}}^*$  with improved feasibility and optimality. This warm-starting approach is fully parallelizable for both diffusion sampling and the solving process of  $\pi$ .

## 4.2 Constrained Diffusion Model

The original diffusion models (DMs) aim to learn the distribution of locally optimal solutions  $p(x^*|y)$  through the loss function in Eq. (5) without knowing any constraint information. As a result, the sampled solutions could be close to the groundtruth but still largely violate the constraints. To address this issue, we propose a novel constrained diffusion model (CDM) to minimize the constraint violations in the sampled trajectories. Inspired by the equation loss in PINN [37], we define a violation function  $V(x, y): \mathcal{X} \times \mathcal{Y} \rightarrow \mathbb{R}$  for differentiable constraints in Eq. (1):

$$V = \sum_{i=1}^l \max(g_i, 0) + \sum_{j=1}^m |h_j|, \quad (6)$$

where  $V(\cdot, \cdot) \in C^1(\mathbb{R}^n, \mathbb{R}^k; \mathbb{R})$  (differentiable except at  $g_i = 0$  or  $h_j = 0$ ) maps from a sample  $x$  and parameter  $y$  and outputs the total constraint violation as a scalar value. In fact, each constraint term can be further customized with different weights that allow different treatments. The violation value is expected to decrease during the training process of diffusion models. We introduce the newly proposed loss function and the corresponding training process as follows.

**CDM Training.** We define the locally optimal solution  $x^* = x_0$  as initial sample in the diffusion process with diffusion step  $k = 0$ . By reformulating the forward sampling process as in Eq. (3), we have  $x_0 = \frac{x_k - \sqrt{1 - \alpha_k} \varepsilon}{\sqrt{\alpha_k}}, \varepsilon \sim \mathcal{N}(0, \mathbf{I})$ . The noise  $\varepsilon$  is approximated as  $\varepsilon_\theta(x_k, k, y)$  with neural-network parameterization. Therefore, we can predict initial sample as  $\hat{x}_0 = \frac{x_k(x_0, \varepsilon) - \sqrt{1 - \alpha_k} \varepsilon_\theta(x_k, k, y)}{\sqrt{\alpha_k}}$ . Then we introduce a constraint violation loss  $\mathcal{L}_{\text{vio}}$  on the predicted  $\hat{x}_0$  from  $x_k, \forall k \in [K]$ :

$$\mathcal{L}_{\text{vio}} = \mathbb{E}_{(x_0, y) \sim \mathcal{X} \times \mathcal{Y}, k \in [K], \varepsilon \sim \mathcal{N}(0, \mathbf{I})} \left[ \frac{1}{k} V \left( \text{clip}(\hat{x}_0(x_k, \varepsilon), x_0^{\min}, x_0^{\max}), y \right) \right] \quad (7)$$

where  $x_0^{\min}$  and  $x_0^{\max}$  are the lower and upper bound for  $x_0 \in \mathcal{X}$ . The reason for the clipping is that at the early phase of the training, the parameterized  $\varepsilon_\theta$  as an approximation of  $\varepsilon$  is not accurate thus the predicted  $\hat{x}_0$  may not lie on the original range of the data  $x_0$ . Therefore, we clip  $\hat{x}_0$  to maintain its range, which guarantees the valid calculation of violation function  $V(\cdot, \cdot)$ . The scheduling factor  $\frac{1}{k}$  regulates

the scale of the violation function  $V$  for different  $x_k, k \in [K]$ . The reason is that the predicted  $\hat{x}_0$  will be more noisy when  $k$  is large therefore the estimation of violation function can be less reliable. This may not be a theoretically principled choice but is found effective and convenient in our experiments.

For the violation loss  $\mathcal{L}_{\text{vio}}$ , we always let the condition variable  $y$  appear in the noise prediction  $\varepsilon_\theta(x_k, k, y)$  without masking it out, contrary to the probabilistic masking in the original training loss  $\mathcal{L}_{\text{diff}}$ . An intuitive interpretation of the additional loss term is that it guides the diffusion model training with the gradients of minimizing the violation value for each denoising step.

Finally, our proposed constrained diffusion training loss is a combination of the original diffusion model training loss and the above violation loss:

$$\mathcal{L} = \mathcal{L}_{\text{diff}} + \lambda \mathcal{L}_{\text{vio}} \quad (8)$$

where  $\lambda$  is a hyperparameter for adjusting the strength of  $\mathcal{L}_{\text{vio}}$ . As the training proceeds, the original loss function  $\mathcal{L}_{\text{diff}}$  will encourage  $\hat{x}_0$  to be close to true  $x_0$ , and  $\mathcal{L}_{\text{vio}}$  further enforces the constraint satisfaction of the generated samples.

**Conditional Diffusion Sampling.** For sampling from trained diffusion models, we adopt guided sampling with classifier-free guidance as introduced in Sec. 3. The guided prediction noise with guidance weight  $c$  is:

$$\hat{\varepsilon}_\theta \leftarrow c \cdot \varepsilon_\theta(x_k, k, y) + (1 - c) \cdot \varepsilon_\theta(x_k, k, \emptyset) \quad (9)$$

Then we plug  $\hat{\varepsilon}_\theta$  into  $\varepsilon_\theta$  in the sampling process [21, 22], and through iterative sampling  $x_{k-1}$  from  $x_k (k = K, \dots, 1)$  with initial random noise  $x_K \sim \mathcal{N}(0, \mathbf{I})$ , it produces the generated samples  $x_0$ . This diffusion samples serve as the predicted initial guess in Sec. 4.1 for a new task:  $\hat{x}_{\text{new}}^* := x_0$ .

## 5 Experiment

In this section, we evaluate the proposed framework combining diffusion models and numerical solvers on three trajectory optimization tasks, and compare with several baselines. Our methods include two DMs: the vanilla diffusion model (DM) and the constrained diffusion model (CDM) as proposed in Sec. 4.2. The experiments involve three stages: 1. Collect solutions provided by numerical solvers on each task domain; 2. For data-driven methods, train the models to fit the solution dataset; 3. For unseen new tasks within each domain, sample initial solutions from models and feed into numerical solvers for deriving final solutions. The details of data collection and model training refer to Appendix A.

**Tasks.** Our experiments are conducted on three trajectory optimization tasks across different domains with examples, as shown in Fig. 1. With an increasing complexity (non-convexity) of the problem, we introduce: (i). *tabletop manipulation* for object relocation with a robotic arm (Sec. 5.1); (ii). the *two-car reach-avoid* problem as a two-player motion planning game (Sec. 5.2); and (iii) the *cislunar transfer* problem for optimal control of the spacecraft (Sec. 5.3). Each task has various DoF, which is derived with the number of control variables at each time step multiplied with the number of discretized steps along the trajectory. The *tabletop manipulation* has a higher DoF due to a larger number of time step ( $T = 80$ ), however, the task is less complex as the *cislunar transfer*, which has more complicated dynamics thus higher non-convexity. More details for each task refer to Appendix A.

**Numerical Solvers.** We assume fully known dynamics and environment for the open-loop optimal control problem. To solve the *tabletop manipulation* and *two-car reach-avoid* problem, we formulate and solve the problem with Sparse Nonlinear OPTimizer (SNOPT) [19] as the solver  $\pi$ , which uses the SQP method and supports warm-starting. For the *cislunar transfer*, we formulate and solve the problem with *pydylan*, a Python interface of the Dynamically Leveraged Automated (N) Multibody Trajectory Optimization (DyLAN) [3] together with SNOPT. The detailed problem formulation and solving for each task are included in Appendix A.

**Baselines.** For comparison with the proposed framework, we introduce the following baselines:

- **Uniform:** This method solely uses a numerical solver with uniformly sampled initial guesses  $x \in \mathcal{X}$  for the non-convex trajectory optimization problem. It solves problems from scratch without leveraging any problem-specific prior information.

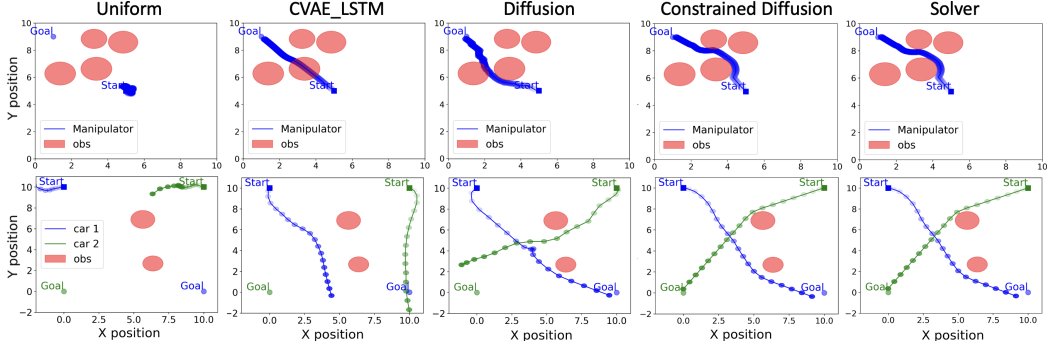


Figure 3: Raw trajectory prediction output and the solver output for the *tabletop manipulation* (top row) and *two-car reach-avoid* problem (bottom row). From left to right, uniform sampling, CVAE\_LSTM, DM, CDM and solver refined locally optimal solution from CDM sampled initial guess.

- **Optimal Uniform:** This method uniformly samples from collected locally optimal solutions  $\{x^*\}$  as initial guesses for the numerical solver, without using any machine learning method to approximate the solution distribution.
- **CVAE\_LSTM:** This method [32] combines the convolutional variational auto-encoder (CVAE) with long short-term memory (LSTM) to learn the conditional distribution of locally optimal solutions. Specifically, a CVAE with Gaussian Mixture Model (GMM) prior is first used to sample the non-control variables, e.g. time or mass variables, and then an LSTM is adapted to sample the control sequence.

Although there exist other graph-based path planning methods like Rapidly-exploring Random Trees (RRT) [31], A\* [20], etc., they can not account for both complex dynamical and environment constraints and flexible optimization objectives in the optimal control problem. Consequently, the comparison against them is not provided in our experiments.

**Diversity Measure.** Apart from the time consumption for deriving feasible solutions, we also apply diversity measure for each method since there exist multiple local optima for each task. Specifically, the Vendi Score [18] is applied to measure the diversity of the model outputs. The similarity kernel we choose is  $k(x, y) = e^{-\|x-y\|}$ .

## 5.1 Tabletop Manipulation

**Task Setting.** For a robotic arm manipulating objects on the tabletop as shown in Fig. 6 in the Appendix, it is important to plan a desired trajectory with goal-reaching and obstacle avoidance. We define the states of the system to be the location of the gripper:  $(p_x, p_y) \in [0, 10]^2$ . In a simplified simulation setting, the movement of the gripper is modeled with linear dynamics  $\dot{p}_x = v_x, \dot{p}_y = v_y$ , where  $u = (v_x, v_y), v_x, v_y \in [-1, 1]$  are two-dimensional speed control variable. In this task  $\mathcal{P}_y$ , we aim to minimize the time for the gripper to reach the goal while avoiding the obstacles.

**Results.** In the top row of Fig. 3, our proposed constrained diffuse model generates a nearly collision-free trajectory to reach the goal, which is very similar to the final refined solution from the solver. The DM tries to navigate through the cluttered environment but chooses a path that inevitably collides with obstacles. The baseline CVAE\_LSTM is not able to account for both goal-reaching and obstacle avoidance. This can be further verified by checking the constraint violation in Table 2, where both DM and CDM achieve significant reduction on constraint violation. CDM has the lowest violation, which justifies the effectiveness of the additional constraint violation loss for training.

When we use our proposed models to warm-start the solver  $\pi$ , only minor refinement is needed to derive locally optimal trajectories. We compute the ratio of locally optimal solutions obtained from 600 initial guesses and present the corresponding time consumption (involving both sampling time from the model and numerical solver time) statistics in Table 1. As demonstrated in Table 1, the CDM with the solver is 29.6 times faster than the uniform method based on the top 25%-quantile of the computational time for deriving the locally optimal solutions. This is further demonstrated in Fig. 5(a)

TASK	METHOD	RATIO	MEAN( $\pm$ STD)	25%-QUANTILE	MEDIAN	VENDI SCORE
TABLETOP	CDM (OURS)	59%	<b>7.29 <math>\pm</math> 16.57</b>	<b>0.50</b>	<b>1.26</b>	5190.70
	DM (OURS)	60%	7.51 $\pm$ 17.50	0.73	1.37	<b>5306.18</b>
	CVAE_LSTM	53%	8.53 $\pm$ 20.87	1.10	1.55	516.61
	UNIFORM	62%	31.65 $\pm$ 24.55	14.81	22.72	<b>5917.73</b>
	OPTIMAL UNIFORM	<b>77%</b>	12.80 $\pm$ 17.70	4.11	7.17	3708.58
TWO-CAR	CDM (OURS)	<b>95%</b>	<b>17.86 <math>\pm</math> 14.28</b>	<b>7.68</b>	<b>13.83</b>	<b>3873.60</b>
	DM (OURS)	<b>95%</b>	18.82 $\pm$ 14.33	8.77	15.61	3574.66
	CVAE_LSTM	63%	36.24 $\pm$ 20.55	19.45	33.26	1162.72
	UNIFORM	64%	46.17 $\pm$ 20.63	29.62	43.54	<b>5256.75</b>
	OPTIMAL UNIFORM	83%	25.15 $\pm$ 19.75	10.82	20.89	3708.58
CISLUNAR	DM (OURS)	<b>54%</b>	<b>50.81 <math>\pm</math> 70.30</b>	<b>9.97</b>	<b>26.68</b>	<b>5999.96</b>
	CVAE_LSTM	30%	141.31 $\pm$ 125.60	38.41	106.48	1403.38
	UNIFORM	18%	199.34 $\pm$ 116.59	114.02	174.35	<b>6000</b>
	OPTIMAL UNIFORM	23%	177.35 $\pm$ 123.22	70.03	153.97	5918.08

Table 1: The ratio of locally optimal solutions, the statistics (mean, standard deviation, quantile and median) of total time consumption including both model sampling time and solver time, and Vendi scores for diversity of sampled trajectories before feeding to the solver.

TASK	METHOD	MEAN( $\pm$ STD)
TABLETOP	CDM (OURS)	<b>4.60 <math>\pm</math> 5.38</b>
	DM (OURS)	4.73 $\pm$ 5.73
	CVAE_LSTM	9.11 $\pm$ 8.16
	UNIFORM	32.20 $\pm$ 3.73
	OPTIMAL UNIFORM	65.44 $\pm$ 40.22
TWO-CAR	CDM (OURS)	<b>3.00 <math>\pm</math> 15.36</b>
	DM (OURS)	10.99 $\pm$ 35.59
	CVAE_LSTM	282.72 $\pm$ 186.40
	UNIFORM	545.66 $\pm$ 294.71
	OPTIMAL UNIFORM	3.27 $\pm$ 3.57

Table 2: The constraint violation value for generated samples before feeding to the solver.

with the solving time histogram of locally optimal solutions, where the CDM with the solver starts to obtain many solutions in a shorter solving time. Then Vendi score result in Table 1 verifies the diversity of our model output, where uniform samples intrinsically have the highest diversity. Thus both efficiency and solution quality are achieved with our framework.

## 5.2 Two-Car Reach-Avoid

**Task settings.** The *two-car reach-avoid* problem is a two-player game where each car tries to find a minimum-time path to reach the goal while avoiding collision with another car and obstacles simultaneously. Specifically, both  $car_1$  and  $car_2$  follows the same dynamics as follows:

$$\dot{p}_x = v \cos \theta, \quad \dot{p}_y = v \sin \theta, \quad \dot{v} = a, \quad \dot{\theta} = \omega,$$

where  $(p_x, p_y, v, \theta)$  denotes the state of each car.  $p_x, p_y$  are the position,  $v$  is the speed, and  $\theta$  is the orientation of the car. Each car has two-dimensional controls  $u^1 = (a^1, \omega^1), u^2 = (a^2, \omega^2)$ , where  $a \in [-1, 1]$  is the acceleration and  $\omega \in [-1, 1]$  is the angular speed. The task setup can be seen in Fig. 1.

**Results.** In the bottom row of Fig. 3, the proposed CDM generates the best prediction of the trajectory solution conditioned on obstacle information  $y$ , which is very close to the final locally optimal solutions refined by the solver. The unconstrained DM samples reasonable trajectory solution prediction, but with much higher constraint violation. The baseline CVAE\_LSTM cannot generate solutions toward goal-reaching. Uniformly sampled initial guesses are usually far from a constraint-satisfying trajectory.

We also evaluate the solving time of obtaining those locally optimal solutions  $x^*$  from the solver  $\pi$  for these five methods in Table 1, and visualize the corresponding histogram in Fig. 5(b). Our proposed CDMs obtained the greatest number of locally optimal solutions from 600 samples as initializations. It is also 3.9 times faster than the uniform method according to the 25%-quantile of the computational time for deriving the locally optimal solutions.



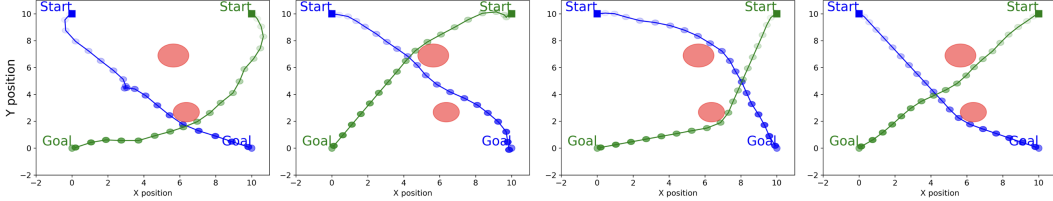


Figure 4: Visualization of four solutions for one *two-car reach-avoid* problem, with CDM predicted initial guesses refined by the solver  $\pi$ .

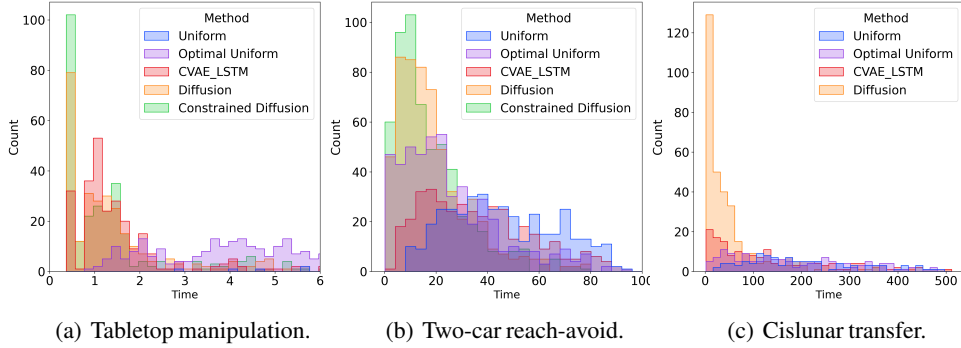


Figure 5: The histogram of total computational time (including model sampling time plus solver time) for different methods to find locally optimal solutions.

To further compare the CDM and the unconstrained DM, we also measure the constraint violation (as defined by Eq. (6)) of all the model outputs in Table 2. Our CDM achieves the lowest constraint violation among all data-driven models. Note that the optimal uniform also achieves small violation because in this task the goal conditions are fixed, the pre-collected solutions will only incur obstacle collision costs which are distance to the obstacle boundary and are inherently small.

The Vendi score in Table 1 shows the superiority of using diffusion models to generate diverse outputs compared to the baseline CVAE\_LSTM. We also visualize the qualitatively different trajectory solution with the proposed CDM and the corresponding solver in Figure 4.

### 5.3 Cislunar Transfer

**Task settings.** In this task, we consider a minimum-fuel *cislunar transfer* with the dynamical model to be a Circular Restricted Three-Body Problem (CR3BP) [27]. Assuming the mass of the spacecraft is negligible, CR3BP describes the equation of motions of a spacecraft under the gravitational force from the sun and moon. Let  $m_1$  be the mass of the Earth and  $m_2$  be the mass of the moon, and  $\mu = m_2/(m_1 + m_2)$ , the dynamics of the spacecraft in the CR3BP is as follows:

$$\ddot{x} - 2\dot{y} = -\bar{U}_x, \quad \ddot{y} + 2\dot{x} = -\bar{U}_y, \quad \ddot{z} = -\bar{U}_z,$$

where  $\bar{U}(r_1(x, y, z), r_2(x, y, z)) = -\frac{1}{2}((1-\mu)r_1^2 + \mu r_2^2) - \frac{1-\mu}{r_1} - \frac{\mu}{r_2}$  represents the effective gravitational potential,  $r_1 = \sqrt{(x+\mu)^2 + y^2 + z^2}$  and  $r_2 = \sqrt{(x-(1-\mu))^2 + y^2 + z^2}$  are the distance from the spacecraft to the sun and moon, respectively. The objective is to minimize fuel expenditure.

**Results.** The *cislunar transfer* is a challenging problem to solve that requires intensive computational time. In Table 1, our method with the unconstrained DM has a huge improvement in the average solving time and the number of locally optimal solutions obtained, compared to the baseline. It is also 7.0 times faster than the uniform method based on the 25%-quantile of computational time for deriving the locally optimal solutions. This can be further verified by the solving time histogram in Fig. 5(c). This improvement encourages us to set a short cut-off time for the solver and use more

time to sample different initial guesses, which further improves the efficiency of obtaining solutions. Finally, the Vendi score shown in Table 1 indicates that our unconstrained DM generates much more diverse predictions than CVAE\_LSTM. Since the *cislunar transfer* task uses a complex numerical integration method for the dynamics constraint which requires extra effort to incorporate it into the neural network, we will leave the CDM for this task as future work.

## 6 Conclusion and Discussion

This paper presents a general and parallelizable framework for non-convex trajectory optimization, using a novel constrained diffusion model combined with numerical solvers. It efficiently provides diverse solutions for problems with multiple local optima, with less constraint violation, and up to 30 times acceleration. It is a general acceleration framework for solving scientific optimization problems.

Limitations also exist for the current framework. Although most constraint functions in trajectory optimization are differentiable (almost everywhere), current CDM does not work for non-differentiable violation functions. For non-differentiable constraints, transforming them into differentiable functions or applying approximation with appropriate bump functions or neural networks is possible. Another problem is that the diffusion sampling may not be achieved in real time in a highly dynamic environment, which can be improved with stride sampling, DDIM [40], etc.

## References

- [1] Ajay, A., Du, Y., Gupta, A., Tenenbaum, J., Jaakkola, T., and Agrawal, P. (2022). Is conditional generative modeling all you need for decision-making? *arXiv preprint arXiv:2211.15657*.
- [2] Amos, B. et al. (2023). Tutorial on amortized optimization. *Foundations and Trends® in Machine Learning*, 16(5):592–732.
- [3] Beeson, R., Sinha, A., Jagannatha, B., Bunce, D., and Carroll, D. (2022). Dynamically leveraged automated multibody (n) trajectory optimization. In *AAS/AIAA Space Flight Mechanics Conference*, Charlotte, NC. American Astronautical Society.
- [4] Betts, J. T. (1998). Survey of numerical methods for trajectory optimization. *Journal of Guidance, Control, and Dynamics*, 21(2):193–207.
- [5] Boggs, P. T. and Tolle, J. W. (1995). Sequential quadratic programming. *Acta numerica*, 4:1–51.
- [6] Botteghi, N., Califano, F., Poel, M., and Brune, C. (2023). Trajectory generation, control, and safety with denoising diffusion probabilistic models. *arXiv preprint arXiv:2306.15512*.
- [7] Cai, S., Mao, Z., Wang, Z., Yin, M., and Karniadakis, G. E. (2021). Physics-informed neural networks (pinns) for fluid mechanics: A review. *Acta Mechanica Sinica*, 37(12):1727–1738.
- [8] Carvalho, J., Le, A. T., Baierl, M., Koert, D., and Peters, J. (2023). Motion planning diffusion: Learning and planning of robot motions with diffusion models. In *2023 IEEE/RSJ International Conference on Intelligent Robots and Systems (IROS)*, pages 1916–1923. IEEE.
- [9] Cauligi, A., Culbertson, P., Schmerling, E., Schwager, M., Stellato, B., and Pavone, M. (2021). Coco: Online mixed-integer control via supervised learning. *IEEE Robotics and Automation Letters*, 7(2):1447–1454.
- [10] Chang, J., Ryu, H., Kim, J., Yoo, S., Seo, J., Prakash, N., Choi, J., and Horowitz, R. (2023). Denoising heat-inspired diffusion with insulators for collision free motion planning. *arXiv preprint arXiv:2310.12609*.
- [11] Chen, S. W., Wang, T., Atanasov, N., Kumar, V., and Morari, M. (2022). Large scale model predictive control with neural networks and primal active sets. *Automatica*, 135:109947.
- [12] Chi, C., Feng, S., Du, Y., Xu, Z., Cousineau, E., Burchfiel, B., and Song, S. (2023). Diffusion policy: Visuomotor policy learning via action diffusion. *arXiv preprint arXiv:2303.04137*.
- [13] Dhariwal, P. and Nichol, A. (2021). Diffusion models beat gans on image synthesis. *Advances in neural information processing systems*, 34:8780–8794.
- [14] Ding, Z. and Jin, C. (2023). Consistency models as a rich and efficient policy class for reinforcement learning. *arXiv preprint arXiv:2309.16984*.
- [15] Ding, Z., Zhang, A., Tian, Y., and Zheng, Q. (2024). Diffusion world model. *arXiv preprint arXiv:2402.03570*.
- [16] Donti, P. L., Rolnick, D., and Kolter, J. Z. (2021). Dc3: A learning method for optimization with hard constraints. *arXiv preprint arXiv:2104.12225*.
- [17] Fehlberg, E. (1969). Klassische runge-kutta-formeln fünfter und siebenter ordnung mit schrittweiten-kontrolle. *Computing*, 4(2):93–106.
- [18] Friedman, D. and Dieng, A. B. (2022). The vendi score: A diversity evaluation metric for machine learning. *arXiv preprint arXiv:2210.02410*.
- [19] Gill, P. E., Murray, W., and Saunders, M. A. (2005). Snopt: An sqp algorithm for large-scale constrained optimization. *SIAM review*, 47(1):99–131.
- [20] Hart, P. E., Nilsson, N. J., and Raphael, B. (1968). A formal basis for the heuristic determination of minimum cost paths. *IEEE transactions on Systems Science and Cybernetics*, 4(2):100–107.

- [21] Ho, J., Jain, A., and Abbeel, P. (2020). Denoising diffusion probabilistic models. *Advances in neural information processing systems*, 33:6840–6851.
- [22] Ho, J. and Salimans, T. (2022). Classifier-free diffusion guidance. *arXiv preprint arXiv:2207.12598*.
- [23] Huang, J., Sun, Z., and Yang, Y. (2023). Accelerating diffusion-based combinatorial optimization solvers by progressive distillation. *arXiv preprint arXiv:2308.06644*.
- [24] Janner, M., Du, Y., Tenenbaum, J. B., and Levine, S. (2022). Planning with diffusion for flexible behavior synthesis. *arXiv preprint arXiv:2205.09991*.
- [25] Karush, W. (1939). Minima of functions of several variables with inequalities as side constraints. *M. Sc. Dissertation. Dept. of Mathematics, Univ. of Chicago*.
- [26] Kingma, D. P. and Ba, J. (2014). Adam: A method for stochastic optimization. *arXiv preprint arXiv:1412.6980*.
- [27] Koon, W. S., Lo, M. W., Marsden, J. E., and Ross, S. D. (2000). Dynamical systems, the three-body problem and space mission design. In *Equadiff'99: (In 2 Volumes)*, pages 1167–1181. World Scientific.
- [28] Krishnamoorthy, S., Mashkaria, S. M., and Grover, A. (2023). Diffusion models for black-box optimization. *arXiv preprint arXiv:2306.07180*.
- [29] Kuhn, H. W. and Tucker, A. W. (2013). Nonlinear programming. In *Traces and emergence of nonlinear programming*, pages 247–258. Springer.
- [30] Kumar, A. and Levine, S. (2020). Model inversion networks for model-based optimization. *Advances in Neural Information Processing Systems*, 33:5126–5137.
- [31] LaValle, S. (1998). Rapidly-exploring random trees: A new tool for path planning. *Research Report 9811*.
- [32] Li, A., Sinha, A., and Beeson, R. (2023). Amortized global search for efficient preliminary trajectory design with deep generative models. *arXiv preprint arXiv:2308.03960*.
- [33] Liang, Z., Mu, Y., Ding, M., Ni, F., Tomizuka, M., and Luo, P. (2023). Adaptdiffuser: Diffusion models as adaptive self-evolving planners. *arXiv preprint arXiv:2302.01877*.
- [34] Mishra, U. A., Xue, S., Chen, Y., and Xu, D. (2023). Generative skill chaining: Long-horizon skill planning with diffusion models. In *Conference on Robot Learning*, pages 2905–2925. PMLR.
- [35] Power, T. and Berenson, D. (2023). Constrained stein variational trajectory optimization. *arXiv preprint arXiv:2308.12110*.
- [36] Power, T., Soltani-Zarrin, R., Iba, S., and Berenson, D. (2023). Sampling constrained trajectories using composable diffusion models. In *IROS 2023 Workshop on Differentiable Probabilistic Robotics: Emerging Perspectives on Robot Learning*.
- [37] Raissi, M., Perdikaris, P., and Karniadakis, G. E. (2019). Physics-informed neural networks: A deep learning framework for solving forward and inverse problems involving nonlinear partial differential equations. *Journal of Computational physics*, 378:686–707.
- [38] Sambharya, R., Hall, G., Amos, B., and Stellato, B. (2023). End-to-end learning to warm-start for real-time quadratic optimization. In *Learning for Dynamics and Control Conference*, pages 220–234. PMLR.
- [39] Sohl-Dickstein, J., Weiss, E., Maheswaranathan, N., and Ganguli, S. (2015). Deep unsupervised learning using nonequilibrium thermodynamics. In *International conference on machine learning*, pages 2256–2265. PMLR.
- [40] Song, J., Meng, C., and Ermon, S. (2020a). Denoising diffusion implicit models. *arXiv preprint arXiv:2010.02502*.

- [41] Song, Y., Sohl-Dickstein, J., Kingma, D. P., Kumar, A., Ermon, S., and Poole, B. (2020b). Score-based generative modeling through stochastic differential equations. *arXiv preprint arXiv:2011.13456*.
- [42] Sridhar, A., Shah, D., Glossop, C., and Levine, S. (2023). Nomad: Goal masked diffusion policies for navigation and exploration. *arXiv preprint arXiv:2310.07896*.
- [43] Sun, Z. and Yang, Y. (2023). Difusco: Graph-based diffusion solvers for combinatorial optimization. *arXiv preprint arXiv:2302.08224*.
- [44] Tevet, G., Raab, S., Gordon, B., Shafir, Y., Cohen-Or, D., and Bermano, A. H. (2022). Human motion diffusion model. *arXiv preprint arXiv:2209.14916*.
- [45] Trabucco, B., Geng, X., Kumar, A., and Levine, S. (2022). Design-bench: Benchmarks for data-driven offline model-based optimization. In *International Conference on Machine Learning*, pages 21658–21676. PMLR.
- [46] Wang, Z., Hunt, J. J., and Zhou, M. (2022). Diffusion policies as an expressive policy class for offline reinforcement learning. *arXiv preprint arXiv:2208.06193*.
- [47] Wright, S. J. (1997). *Primal-dual interior-point methods*. SIAM.
- [48] Xiao, W., Wang, T.-H., Gan, C., and Rus, D. (2023). Safediffuser: Safe planning with diffusion probabilistic models. *arXiv preprint arXiv:2306.00148*.
- [49] Yang, Z., Mao, J., Du, Y., Wu, J., Tenenbaum, J. B., Lozano-Pérez, T., and Kaelbling, L. P. (2023). Compositional diffusion-based continuous constraint solvers. *arXiv preprint arXiv:2309.00966*.
- [50] Zeilinger, M. N., Jones, C. N., and Morari, M. (2011). Real-time suboptimal model predictive control using a combination of explicit mpc and online optimization. *IEEE Transactions on Automatic Control*, 56(7):1524–1534.
- [51] Zhang, X., Bujarbaruah, M., and Borrelli, F. (2019). Safe and near-optimal policy learning for model predictive control using primal-dual neural networks. In *2019 American Control Conference (ACC)*, pages 354–359. IEEE.

## A Implementation and Task Details

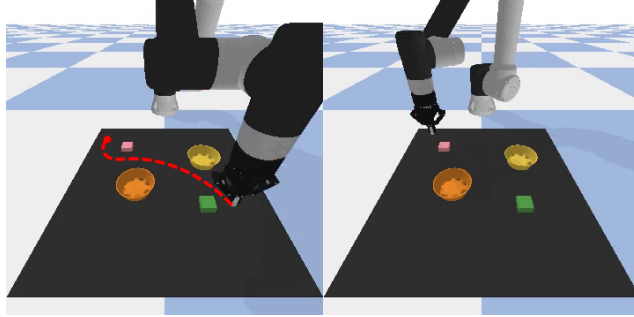
### A.1 Model Details

For both unconstrained and constrained diffusion models, we apply a UNet structure with three hidden layers of 512, 512 and 1024 neurons. We also use a fully connected layer of 256 and 512 neurons to embed the conditional input  $y$ . The sampling step is set to be 500. Both DMs are trained with 200 epochs using the Adam optimizer [26]. The constrained and unconstrained DMs usually take 14 hours and 6 hours respectively, as well as 20 GB VRAM to train on one NVIDIA A100 GPU, respectively.

### A.2 Tabletop Manipulation

**Problem formulation and solving.** In this task  $\mathcal{P}_y$ , we aim to minimize the time for the gripper to reach the goal while avoiding the obstacles. The start position is fixed at (5,5). The conditional parameter  $y$  includes the goal position  $p_{\text{goal}}$  randomly chosen from  $\{(1,1), (1,9), (9,1), (9,9)\}$ , 4 obstacle positions  $p_{\text{obs}}$  randomly sampled between the start and goal, and the obstacle radius  $r_{\text{obs}}$  randomly sampled from  $[0.5, 1.0]$ . We discretize this problem into  $T$  timesteps where  $T = 80$ . The variable to optimize is  $x = (t_{\text{final}}, u_1, u_2, \dots, u_T) \in \mathbb{R}^{161}$ , and the conditional parameter is  $y = (p_{\text{goal}}, p_{\text{obs}}, r_{\text{obs}}) \in \mathbb{R}^{14}$ . The objective is defined as  $J(x; y) = t_{\text{final}}$ . The constraint  $g$  includes the goal-reaching constraints at  $t_{\text{final}}$  and the collision avoidance for obstacles at all time. We use the 4-th order Runge-Kutta (RK4) method to integrate the dynamics and formulate the constraints.

Figure 6: An example of tabletop manipulation task for goal-reaching and obstacle avoidance movement, using a CDM with a numerical solver for planning: (left) starting position of the gripper and the planned trajectory; (right) target position reached by the gripper.



**Data collection and model training.** In this task, to collect the training data we sample 2700 different  $y$ , each with 100 uniformly sampled initial guesses. Then we use the SNOPT [19] solver for each problem instance to collect locally optimal solutions. Finally, we filter out those solutions with objective values greater than 6 s and use the remaining 237k data as training data. Within this 237k data, 10% of the data are used as the validation set. The whole data collection process takes around 15 hours with 200 AMD EPYC 9654 CPU cores.

We train each of our proposed constrained and unconstrained DMs and baseline models with 3 different random seeds. The models are tested for the warm-starting performance with 600 initial guesses from 3 random seeds across 20 unseen locations of the goal and obstacles, i.e. unseen  $y$  values.

### A.3 Two Car Reach-Avoid

**Problem formulation and solving.** In this task  $\mathcal{P}_y$ , we aim to minimize the time for the two cars to reach each own goal while avoiding colliding with the other car and obstacles. We fixed the start  $p_{\text{start}}$  and goal  $p_{\text{goal}}$  position for  $car_1$  to be  $(0, 10)$  and  $(10, 0)$ , and for  $car_2$  to be  $(10, 0)$  and  $(0, 0)$ . The conditional parameters  $y \in \mathbb{R}^6$  include the two obstacle positions  $p_{\text{obs}}$  randomly sampled from  $[2.0, 8.0]$ , and the obstacle radius  $r_{\text{obs}}$  randomly sampled from  $[0.5, 1.5]$ . We formulate this trajectory optimization problem with a forward shooting method, with the discretized time step  $T = 40$ . The variable to optimize is  $x = (t_{\text{final}}, u_1^1, u_2^1, \dots, u_T^1, u_1^2, u_2^2, \dots, u_T^2)$ , where  $u_i^1$  and  $u_i^2$  are controls for two cars, respectively. The problem parameter is  $y = (p_{\text{obs}}, r_{\text{obs}})$ . The objective is defined as  $J(x; y) = t_{\text{final}}$ . The constraint  $g$  includes the goal-reaching constraints at  $t_{\text{final}}$ , and the collision avoidance for obstacles and between each car for all time. We use the 4-th order Runge-Kutta (RK4) method to integrate the dynamics and formulate the constraints.

**Data collection and model training.** In this task, we collect locally optimal solutions  $x^*$  from 3k different  $y$ , each with 100 uniformly sampled initial guesses using SNOPT [19]. We filter out those solutions whose objective is higher than 12 s and use the remaining 114k solutions as the training data. Within this 114k data, 10% of the data are used as the validation set. The whole data collection process takes around 8 hours with 200 AMD EPYC 9654 CPU cores.

We train each of our proposed constrained and unconstrained DMs and baseline models with 3 different random seeds and test the warm-starting performance with 600 initial guesses sampled from 3 random seeds across 20 unseen obstacle settings, i.e. unseen  $y$  values.

### A.4 Cislunar Transfer

**Problem formulation and solving.** In this problem  $\mathcal{P}_y$ , as shown in Fig. 1, the spacecraft is planned to start from a Geostationary Transfer Spiral (blue) and reach a stable manifold arc (green) of a Halo orbit near  $L_1$  Lagrange point (green). A candidate trajectory solution is plotted in orange. The CR3BP is a chaotic system, where a smaller perturbation will lead to a significantly different final trajectory. Therefore, trajectory optimization of this problem contains many local optima. We choose the conditional parameter  $y \in [0.1, 1.0]$  Newton to be the maximum allowable thrust of the spacecraft.

We use the forward-backward shooting method to formulate the trajectory optimization problem in Eq. (1). For the spacecraft, we set the constant specific impulse (CSI)  $I_{sp} = 1000$  s. The initial dry mass is 300 kg and the initial fuel mass is 700 kg. We choose  $T$  discretized control segments where  $T = 20$

and the control  $u$  are uniformly applied on each segment. The variable  $x$  to optimize is as follows:

$$\mathbf{x} = (t_{\text{burn}}, t_{\text{coast}}^{\text{initial}}, t_{\text{coast}}^{\text{final}}, m_f, u_1, u_2, \dots, u_N) \quad (10)$$

where  $t_{\text{burn}}, t_{\text{coast}}^{\text{initial}}, t_{\text{coast}}^{\text{final}}$  are the effective burning time for the engine, initial and final coast time,  $m_f$  is the final mass, and  $u_i$  is a three-dimensional thrust control of the spacecraft. The objective is defined as  $J(x; y) = -m_f$ , which is to minimize fuel expenditure. The constraint  $g$  is the midpoint agreement when integrating dynamics from forward and backward. The problem parameter  $y$  is the maximum allowable thrust for the spacecraft and is bounded by  $[0.1, 1]$  Newton. To integrate the dynamics, we use the Runge-Kutta-Fehlberg 5-4th order (RK54) method [17].

**Data collection and model training.** To collect the training data, we sample 12 different  $y$  values from a grid in  $[0.1, 1]$  Newton, and for each  $y$  we collect 25k locally optimal solutions with  $m_f \geq 415\text{kg}$  total amount of 300k data. The problem is solved using *pydylan*, a python interface of the Dynamically Leveraged Automated (N) Multibody Trajectory Optimization (DyLAN) [3] and the solver SNOPT [19]. Within this 300k data, 10% of the data are used as the validation set. The whole data collection process takes around 3 days with 500 Intel Skylake CPU cores.

We train the unconstrained DM and baseline models on 3 random seeds, and we test the warm-starting performance with 600 initial guesses sampled from 3 random seeds on  $y = 0.15$  Newton, which is unseen in training data.

## NeurIPS Paper Checklist

### 1. Claims

Question: Do the main claims made in the abstract and introduction accurately reflect the paper's contributions and scope?

Answer: [Yes]

Justification: The abstract and introduction clearly reflect the paper's contributions and scope.

Guidelines:

- The answer NA means that the abstract and introduction do not include the claims made in the paper.
- The abstract and/or introduction should clearly state the claims made, including the contributions made in the paper and important assumptions and limitations. A No or NA answer to this question will not be perceived well by the reviewers.
- The claims made should match theoretical and experimental results, and reflect how much the results can be expected to generalize to other settings.
- It is fine to include aspirational goals as motivation as long as it is clear that these goals are not attained by the paper.

### 2. Limitations

Question: Does the paper discuss the limitations of the work performed by the authors?

Answer: [Yes]

Justification: Limitations are discussed in the final sections.

Guidelines:

- The answer NA means that the paper has no limitation while the answer No means that the paper has limitations, but those are not discussed in the paper.
- The authors are encouraged to create a separate "Limitations" section in their paper.
- The paper should point out any strong assumptions and how robust the results are to violations of these assumptions (e.g., independence assumptions, noiseless settings, model well-specification, asymptotic approximations only holding locally). The authors should reflect on how these assumptions might be violated in practice and what the implications would be.
- The authors should reflect on the scope of the claims made, e.g., if the approach was only tested on a few datasets or with a few runs. In general, empirical results often depend on implicit assumptions, which should be articulated.
- The authors should reflect on the factors that influence the performance of the approach. For example, a facial recognition algorithm may perform poorly when image resolution is low or images are taken in low lighting. Or a speech-to-text system might not be used reliably to provide closed captions for online lectures because it fails to handle technical jargon.
- The authors should discuss the computational efficiency of the proposed algorithms and how they scale with dataset size.
- If applicable, the authors should discuss possible limitations of their approach to address problems of privacy and fairness.
- While the authors might fear that complete honesty about limitations might be used by reviewers as grounds for rejection, a worse outcome might be that reviewers discover limitations that aren't acknowledged in the paper. The authors should use their best judgment and recognize that individual actions in favor of transparency play an important role in developing norms that preserve the integrity of the community. Reviewers will be specifically instructed to not penalize honesty concerning limitations.

### 3. Theory Assumptions and Proofs

Question: For each theoretical result, does the paper provide the full set of assumptions and a complete (and correct) proof?

Answer: [NA]



Justification: No theory results

Guidelines:

- The answer NA means that the paper does not include theoretical results.
- All the theorems, formulas, and proofs in the paper should be numbered and cross-referenced.
- All assumptions should be clearly stated or referenced in the statement of any theorems.
- The proofs can either appear in the main paper or the supplemental material, but if they appear in the supplemental material, the authors are encouraged to provide a short proof sketch to provide intuition.
- Inversely, any informal proof provided in the core of the paper should be complemented by formal proofs provided in appendix or supplemental material.
- Theorems and Lemmas that the proof relies upon should be properly referenced.

#### 4. **Experimental Result Reproducibility**

Question: Does the paper fully disclose all the information needed to reproduce the main experimental results of the paper to the extent that it affects the main claims and/or conclusions of the paper (regardless of whether the code and data are provided or not)?

Answer: [Yes]

Justification: The paper disclose all information for the main experiment results.

Guidelines:

- The answer NA means that the paper does not include experiments.
- If the paper includes experiments, a No answer to this question will not be perceived well by the reviewers: Making the paper reproducible is important, regardless of whether the code and data are provided or not.
- If the contribution is a dataset and/or model, the authors should describe the steps taken to make their results reproducible or verifiable.
- Depending on the contribution, reproducibility can be accomplished in various ways. For example, if the contribution is a novel architecture, describing the architecture fully might suffice, or if the contribution is a specific model and empirical evaluation, it may be necessary to either make it possible for others to replicate the model with the same dataset, or provide access to the model. In general, releasing code and data is often one good way to accomplish this, but reproducibility can also be provided via detailed instructions for how to replicate the results, access to a hosted model (e.g., in the case of a large language model), releasing of a model checkpoint, or other means that are appropriate to the research performed.
- While NeurIPS does not require releasing code, the conference does require all submissions to provide some reasonable avenue for reproducibility, which may depend on the nature of the contribution. For example
  - (a) If the contribution is primarily a new algorithm, the paper should make it clear how to reproduce that algorithm.
  - (b) If the contribution is primarily a new model architecture, the paper should describe the architecture clearly and fully.
  - (c) If the contribution is a new model (e.g., a large language model), then there should either be a way to access this model for reproducing the results or a way to reproduce the model (e.g., with an open-source dataset or instructions for how to construct the dataset).
  - (d) We recognize that reproducibility may be tricky in some cases, in which case authors are welcome to describe the particular way they provide for reproducibility. In the case of closed-source models, it may be that access to the model is limited in some way (e.g., to registered users), but it should be possible for other researchers to have some path to reproducing or verifying the results.

#### 5. **Open access to data and code**

Question: Does the paper provide open access to the data and code, with sufficient instructions to faithfully reproduce the main experimental results, as described in supplemental material?

Answer: [No]

Justification: Currently the code and data are not provided. The results are reproducible.

Guidelines:

- The answer NA means that paper does not include experiments requiring code.
- Please see the NeurIPS code and data submission guidelines (<https://nips.cc/public/guides/CodeSubmissionPolicy>) for more details.
- While we encourage the release of code and data, we understand that this might not be possible, so “No” is an acceptable answer. Papers cannot be rejected simply for not including code, unless this is central to the contribution (e.g., for a new open-source benchmark).
- The instructions should contain the exact command and environment needed to run to reproduce the results. See the NeurIPS code and data submission guidelines (<https://nips.cc/public/guides/CodeSubmissionPolicy>) for more details.
- The authors should provide instructions on data access and preparation, including how to access the raw data, preprocessed data, intermediate data, and generated data, etc.
- The authors should provide scripts to reproduce all experimental results for the new proposed method and baselines. If only a subset of experiments are reproducible, they should state which ones are omitted from the script and why.
- At submission time, to preserve anonymity, the authors should release anonymized versions (if applicable).
- Providing as much information as possible in supplemental material (appended to the paper) is recommended, but including URLs to data and code is permitted.

## 6. Experimental Setting/Details

Question: Does the paper specify all the training and test details (e.g., data splits, hyperparameters, how they were chosen, type of optimizer, etc.) necessary to understand the results?

Answer: [Yes]

Justification: The experiment settings are stated in the main text and the appendix.

Guidelines:

- The answer NA means that the paper does not include experiments.
- The experimental setting should be presented in the core of the paper to a level of detail that is necessary to appreciate the results and make sense of them.
- The full details can be provided either with the code, in appendix, or as supplemental material.

## 7. Experiment Statistical Significance

Question: Does the paper report error bars suitably and correctly defined or other appropriate information about the statistical significance of the experiments?

Answer: [Yes]

Justification: The experiment analysis shows the statistical significance of the results.

Guidelines:

- The answer NA means that the paper does not include experiments.
- The authors should answer "Yes" if the results are accompanied by error bars, confidence intervals, or statistical significance tests, at least for the experiments that support the main claims of the paper.
- The factors of variability that the error bars are capturing should be clearly stated (for example, train/test split, initialization, random drawing of some parameter, or overall run with given experimental conditions).
- The method for calculating the error bars should be explained (closed form formula, call to a library function, bootstrap, etc.)
- The assumptions made should be given (e.g., Normally distributed errors).
- It should be clear whether the error bar is the standard deviation or the standard error of the mean.

- It is OK to report 1-sigma error bars, but one should state it. The authors should preferably report a 2-sigma error bar than state that they have a 96% CI, if the hypothesis of Normality of errors is not verified.
- For asymmetric distributions, the authors should be careful not to show in tables or figures symmetric error bars that would yield results that are out of range (e.g. negative error rates).
- If error bars are reported in tables or plots, The authors should explain in the text how they were calculated and reference the corresponding figures or tables in the text.

## 8. Experiments Compute Resources

Question: For each experiment, does the paper provide sufficient information on the computer resources (type of compute workers, memory, time of execution) needed to reproduce the experiments?

Answer: [Yes]

Justification: The computational resources are provided in the main text and appendix.

Guidelines:

- The answer NA means that the paper does not include experiments.
- The paper should indicate the type of compute workers CPU or GPU, internal cluster, or cloud provider, including relevant memory and storage.
- The paper should provide the amount of compute required for each of the individual experimental runs as well as estimate the total compute.
- The paper should disclose whether the full research project required more compute than the experiments reported in the paper (e.g., preliminary or failed experiments that didn't make it into the paper).

## 9. Code Of Ethics

Question: Does the research conducted in the paper conform, in every respect, with the NeurIPS Code of Ethics <https://neurips.cc/public/EthicsGuidelines>?

Answer: [Yes]

Justification: The research conforms with the NeurIPS Code of Ethics.

Guidelines:

- The answer NA means that the authors have not reviewed the NeurIPS Code of Ethics.
- If the authors answer No, they should explain the special circumstances that require a deviation from the Code of Ethics.
- The authors should make sure to preserve anonymity (e.g., if there is a special consideration due to laws or regulations in their jurisdiction).

## 10. Broader Impacts

Question: Does the paper discuss both potential positive societal impacts and negative societal impacts of the work performed?

Answer: [NA]

Justification: This paper focuses on solving a mathematical optimization problem and the application will not have societal impacts such as disinformation, fairness or privacy.

Guidelines:

- The answer NA means that there is no societal impact of the work performed.
- If the authors answer NA or No, they should explain why their work has no societal impact or why the paper does not address societal impact.
- Examples of negative societal impacts include potential malicious or unintended uses (e.g., disinformation, generating fake profiles, surveillance), fairness considerations (e.g., deployment of technologies that could make decisions that unfairly impact specific groups), privacy considerations, and security considerations.

- The conference expects that many papers will be foundational research and not tied to particular applications, let alone deployments. However, if there is a direct path to any negative applications, the authors should point it out. For example, it is legitimate to point out that an improvement in the quality of generative models could be used to generate deepfakes for disinformation. On the other hand, it is not needed to point out that a generic algorithm for optimizing neural networks could enable people to train models that generate Deepfakes faster.
- The authors should consider possible harms that could arise when the technology is being used as intended and functioning correctly, harms that could arise when the technology is being used as intended but gives incorrect results, and harms following from (intentional or unintentional) misuse of the technology.
- If there are negative societal impacts, the authors could also discuss possible mitigation strategies (e.g., gated release of models, providing defenses in addition to attacks, mechanisms for monitoring misuse, mechanisms to monitor how a system learns from feedback over time, improving the efficiency and accessibility of ML).

### 11. Safeguards

Question: Does the paper describe safeguards that have been put in place for responsible release of data or models that have a high risk for misuse (e.g., pretrained language models, image generators, or scraped datasets)?

Answer: [NA]

Justification: This paper doesn't pose such risks.

Guidelines:

- The answer NA means that the paper poses no such risks.
- Released models that have a high risk for misuse or dual-use should be released with necessary safeguards to allow for controlled use of the model, for example by requiring that users adhere to usage guidelines or restrictions to access the model or implementing safety filters.
- Datasets that have been scraped from the Internet could pose safety risks. The authors should describe how they avoided releasing unsafe images.
- We recognize that providing effective safeguards is challenging, and many papers do not require this, but we encourage authors to take this into account and make a best faith effort.

### 12. Licenses for existing assets

Question: Are the creators or original owners of assets (e.g., code, data, models), used in the paper, properly credited and are the license and terms of use explicitly mentioned and properly respected?

Answer: [Yes]

Justification: The existing assets are properly referenced.

Guidelines:

- The answer NA means that the paper does not use existing assets.
- The authors should cite the original paper that produced the code package or dataset.
- The authors should state which version of the asset is used and, if possible, include a URL.
- The name of the license (e.g., CC-BY 4.0) should be included for each asset.
- For scraped data from a particular source (e.g., website), the copyright and terms of service of that source should be provided.
- If assets are released, the license, copyright information, and terms of use in the package should be provided. For popular datasets, [paperswithcode.com/datasets](https://paperswithcode.com/datasets) has curated licenses for some datasets. Their licensing guide can help determine the license of a dataset.
- For existing datasets that are re-packaged, both the original license and the license of the derived asset (if it has changed) should be provided.
- If this information is not available online, the authors are encouraged to reach out to the asset's creators.

### 13. New Assets

Question: Are new assets introduced in the paper well documented and is the documentation provided alongside the assets?

Answer: [No]

Justification: Currently the paper doesn't release new assets.

Guidelines:

- The answer NA means that the paper does not release new assets.
- Researchers should communicate the details of the dataset/code/model as part of their submissions via structured templates. This includes details about training, license, limitations, etc.
- The paper should discuss whether and how consent was obtained from people whose asset is used.
- At submission time, remember to anonymize your assets (if applicable). You can either create an anonymized URL or include an anonymized zip file.

#### 14. **Crowdsourcing and Research with Human Subjects**

Question: For crowdsourcing experiments and research with human subjects, does the paper include the full text of instructions given to participants and screenshots, if applicable, as well as details about compensation (if any)?

Answer: [NA]

Justification: This paper does not involve crowdsourcing nor research with human subjects.

Guidelines:

- The answer NA means that the paper does not involve crowdsourcing nor research with human subjects.
- Including this information in the supplemental material is fine, but if the main contribution of the paper involves human subjects, then as much detail as possible should be included in the main paper.
- According to the NeurIPS Code of Ethics, workers involved in data collection, curation, or other labor should be paid at least the minimum wage in the country of the data collector.

#### 15. **Institutional Review Board (IRB) Approvals or Equivalent for Research with Human Subjects**

Question: Does the paper describe potential risks incurred by study participants, whether such risks were disclosed to the subjects, and whether Institutional Review Board (IRB) approvals (or an equivalent approval/review based on the requirements of your country or institution) were obtained?

Answer: [NA]

Justification: This paper does not involve crowdsourcing nor research with human subjects.

Guidelines:

- The answer NA means that the paper does not involve crowdsourcing nor research with human subjects.
- Depending on the country in which research is conducted, IRB approval (or equivalent) may be required for any human subjects research. If you obtained IRB approval, you should clearly state this in the paper.
- We recognize that the procedures for this may vary significantly between institutions and locations, and we expect authors to adhere to the NeurIPS Code of Ethics and the guidelines for their institution.
- For initial submissions, do not include any information that would break anonymity (if applicable), such as the institution conducting the review.